Chaos, Solitons and Fractals 187 (2024) 115353

Contents lists available at ScienceDirect

Chaos, Solitons and Fractals

journal homepage: www.elsevier.com/locate/chaos

Qualitative analysis and new variety of solitons profiles for the (1+1)-dimensional modified equal width equation

Syed Asif Ali Shah [a,b,c,*], Ejaz Hussain [d,*], Wen-Xiu Ma [e,f,g,*], Zhao Li [h], Adham E. Ragab [i], Tamer M. Khalaf [i]

[a] University of Science and Technology of China, Hefei 230026, China
[b] Jinhua Hangda Beidou Applied Technology Co., Ltd., Jinhua 321004, China
[c] Department of Mathematics and Statistics, The University of Lahore, 1-km Defence Road, Lahore 54000, Pakistan
[d] Department of Mathematics, University of the Punjab, Quaid-e-Azam Campus, Lahore, 54590, Pakistan
[e] Department of Mathematics, Zhejiang Normal University, Jinhua 321004, China
[f] Department of Mathematics and Statistics, University of South Florida, Tampa, FL 33620, USA
[g] Material Science Innovation and Modelling, Department of Mathematical Sciences, North-West University, Mafikeng Campus, Mmabatho 2735, South Africa
[h] College of Computer Science, Chengdu University, Chengdu, 610106, China
[i] Department of Industrial Engineering, College of Engineering King Saud University, P.O. Box 800, Riyadh 11421, Saudi Arabia

ARTICLE INFO

Keywords:
Modified equal width equation
Modified auxiliary equation method
Bifurcation analysis
Chaotic behavior
Sensitivity and stability analysis

ABSTRACT

The objective of this manuscript is to examine the nonlinear characteristics of the modified equal width equation that is used to simulate the one-dimensional wave propagation nonlinear media, incorporating the dispersion process. Utilizing the traveling wave transformations, we are able to convert the nonlinear partial differential equations (NLPDES) into ordinary differential equations (NLODEs). In this study, an analytical technique is used to utilize the exact soliton solutions of this proposed model. This efficient method is known as the modified auxiliary equation method. This extraction of soliton solutions contains various types of solutions such as trigonometric, hyperbolic, and rational solutions. For a graphical representation, we utilize Mathematica and Maple software to depict the solutions in $3D$, $2D$, contour plots, and density plots. The main novelty of this paper is to explore the qualitative study, which includes the chaotic behavior, bifurcation, sensitivity, and stability analysis of this problem. For this, first, we apply the Galilean transformation, we convert the NLODEs into two systems of equations. Moreover, the qualitative dynamics of the time-varying dynamical system are examined by employing chaos theory. We explore the intricacies of $3D$ and $2D$ phase portraits, time series, and Poincaré maps as powerful tools for detecting the elusive nature of chaos in self-governing dynamic systems. Sensitivity and stability analysis is also studied by using the various initial conditions, revealing the remarkable stability of the system under investigation. The system's stability is confirmed by the fact that even small changes to the initial conditions have no appreciable effect on the solutions. The results of this study are novel and valuable for further investigation of equations which are helpful for the incoming researchers.

1. Introduction

It is generally recognized that nearly all non-linear physical processes may be explained using mathematical equations, often known as non-linear differential equations. Nonlinear phenomena have been extensively explored through the use of models such as nonlinear partial differential equations (NLPDEs), which stand out as being of utmost importance in this field. Nonlinear (PDEs) have proven to be a potent tool in effectively characterizing a vast array of physical phenomena across a diverse range of disciplines [1–4].

In recent years, there has been a particular focus on the modified equal width (MEW) equation involving nonlinear medium and dispersion processes. This has led to a rising interest in the exploration of "exact solutions" for NPDEs. Solitons hold a crucial position within soliton theory, with various types documented in literature

* Corresponding authors.
E-mail addresses: asif.ali@math.uol.edu.pk (S.A.A. Shah), ejazhusain.math@gmail.com (E. Hussain), mawx@cas.usf.edu (W.-X. Ma), lizhao10.26@163.com (Z. Li), aragab@ksu.edu.sa (A.E. Ragab), tamkhalaf@KSU.EDU.SA (T.M. Khalaf).

https://doi.org/10.1016/j.chaos.2024.115353
Received 10 March 2024; Received in revised form 23 July 2024; Accepted 30 July 2024
Available online 8 August 2024

such as dark soliton, bright soliton, singular soliton, and others. Due to their significant mathematical properties and wide-ranging applications, multiple techniques have been proposed to study different physical phenomena related to nonlinear wave equations. It is recognized that the effectiveness of these approaches varies depending on the specific problem at hand; while some techniques are suitable for certain issues, they may not apply to others. The analytical solutions of NPDEs are pivotal in comprehending the qualitative traits and physical implications of numerous phenomena. Various methods have been successfully devised and utilized in the existing literature to derive analytical solutions for NPDEs, such as $(\frac{G'}{G})$ expansion approach [5,6], modified exp-function approach [7], exponential rational function approach [8,9], inverse scattering approach [10], generalized unified approach [11], Hirota bilinear approach [12], simplified Hirota bilinear approach [13], Bäcklund and Darboux transformations approach [14–16], modified auxiliary equation approach [17], modified extended tanh function [18], generalized Kudryashov approach [19], extended algebraic approach [20], extended simple equation approach [21], homogeneous balancing approach [22], planner dynamical system scheme [23,24], and numerous other approaches that have not yet been discovered. The literary canon is full of answers that have been discovered via careful investigation. These astounding answers cover a wide range: they are breather wave solutions to solitary wave solutions, hyperbolic solutions to rogue wave solutions, periodic solutions to logical solutions, and many qualitative analysis [25–40]. One can find different types of solutions are discussed. Notably, solutions such as [41–46] stand out as exceptionally exceptional.

Nonlinear physical systems have experienced a surge in recognition in recent times. Chaos has become more common in models. Qualitative research based on theory [47–53] has become crucial for exploring the structures of dynamical models.

The term "chaos" has been assigned to the occurrence of unpredictable and erratic temporal changes within different nonlinear systems. Chaos is common in nonlinear systems, characterized by the system's inability to repeat its former behavior. Despite its apparent unpredictability, chaotic dynamical systems are governed by deterministic equations. Chaotic systems are set apart by their remarkable sensitivity to initial conditions. The wide number of beginning conditions produces an unmatched variety of orbits. These differences, however, end in almost similar paths in systems devoid of chaos. For chaos to manifest in continuous-time systems, a trinity of independent dynamical variables and nonlinearity must exist. These prerequisites are crucial for detecting chaos in such systems. A chaotic system is defined as one that is highly sensitive to initial conditions. As such, the exact definition of chaos can be stated as follows: A chaotic system is characterized as a coherent system that displays unexpected and random behavior, with its distinctive feature being the fragile reliance on initial conditions. The examination of chaos and the mathematical concepts underpinning it holds significant importance in the twenty-first century.

When bounded solutions diverge locally rather than exhibiting periodic or quasi-periodic behavior, a dynamical system is considered chaotic .

There are various methods for recognizing chaos. This examination identifies the most useful ones. These are as follows:

- Time series,
- Phase portraits,
- Poincaré maps.

The discussion explores a thorough examination of the system sensitivity and stability analysis. The authors claim that this study is a unique and intriguing commitment that is unheard of in the setting of the system in issues. In recent years, there has been a growing trend in subjecting nonlinear physical models to qualitative investigation based on bifurcation [54]. The analysis of bifurcation aims to explore the potential changes in the trajectory of a dynamical system as its parameters undergo variations. Common bifurcation patterns such as pitchfork, saddle–node, and Hopf bifurcations, along with period-doubling bifurcation and bifurcations leading to chaos from quasi-periodic motion, are generally considered to be typical occurrences The current investigation explores the complexities of the Modified Equal Width Equation (MEWE), which can be represented as follows.

$$\mathcal{S}_t + \upsilon \mathcal{S}^2 \mathcal{S}_x - \rho \mathcal{S}_{xxt} = 0, \tag{1.1}$$

here υ and ρ are constant. This particular equation holds immense importance in fluid mechanics and has therefore received much attention from the scientific community. Erudite researchers have undertaken countless studies to delve into the complexities of this equation and its implications on various physical phenomena. Several investigations have been conducted on the MEW equation, yielding diverse results. Wazwaz [55], ingeniously generated a variety of exact solutions for the equation, while Lu [56], employed the variational iteration method to numerically analyze this type of equation. Finite difference method [57], was utilized to derive solitary wave solutions, and a lumped Galerkin method [58], was adopted to numerically tackle the MEWE. Integral bifurcation technique [59], was employed to construct traveling wave solutions of the equation, and exact solutions were found through the $(\frac{G'}{G})$-expansion method [60]. The homotopy perturbation method [61], was applied to present numerical results of the MEWE, while Fourier spectral method [62], was utilized to obtain numerical results. The Exp-function method [63], was used to derive soliton solutions of the MEW equation, and the method of dynamical system [64], was employed to obtain exact solutions.

The manuscript is summarized as follows: Section 2 describes the conversion of the governing model to a reduced form. Section 3 discussed the qualitative analysis like bifurcation and chaotic analysis with $2D$, $3D$ phase portraits, Poincare map, and time series. Sections 4 discussed the sensitivity and stability analysis with phase and group velocity of a wave expatiated. Section 5 describes the structure of different types of soliton profiles and graphical simulation of the obtained result by using the suitable parameter values and the last section discusses the conclusion.

2. Mathematical analysis

General NLPDE has the form

$$\Omega(\mathcal{S}, \mathcal{S}_x, \mathcal{S}_{xx}\mathcal{S}_{xt}, \mathcal{S}_{xxx} \ldots) = 0, \tag{2.1}$$

whereas the function $s = s(x,t)$ remains unknown, the application of the subsequent transformations permits the conversion of the given NLPDE, as denoted by Eq. (1.1), into a nonlinear ODE through the implementation of the ensuing transformation:

$$\mathcal{S}(x,t) = \psi(\zeta), \zeta = x - \omega t. \tag{2.2}$$

In result, ODE of the form

$$\Omega(\psi,\ \psi',\ \psi'',\ \psi''',\ \ldots) = 0. \tag{2.3}$$

To determine the precise solutions of Eq. (1.1), it is imperative to presuppose that the aforementioned equation allows for the implementation of traveling wave transformations. This presupposition is based on the compatibility of Eq. (1.1) with the transformations mentioned.

$$\mathcal{S}(x,t) = \psi(\zeta), \zeta = x - \omega t. \tag{2.4}$$

substitute Eq. (2.2) into Eq. (1.1), we change Eq. (1.1) into ODE of the form

$$-\omega\psi' + \upsilon\psi^2\psi' + \rho\omega\psi''' = 0. \tag{2.5}$$

The result of doing one integration of Eq. (2.5) concerning ζ while setting the integration of constant is equal to zero the following result is obtained:

$$-\omega\psi + \frac{\upsilon}{3}\psi^3 + \rho\omega\psi'' = 0. \tag{2.6}$$

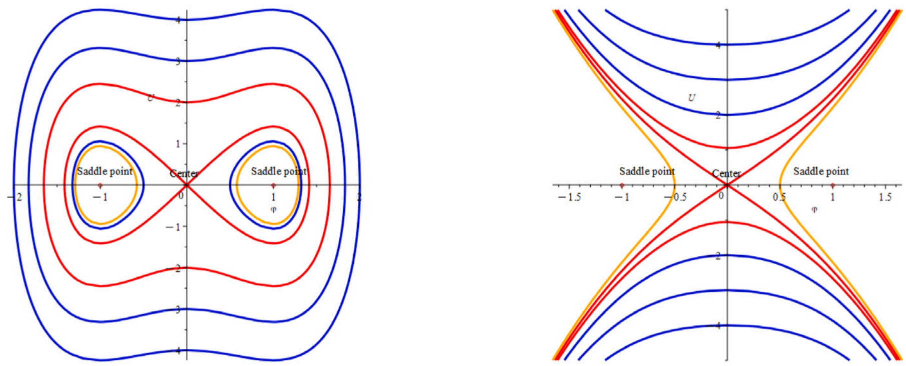

(a) $P > 0$and $Q > 0$ (b) $P > 0$ and $Q < 0$

Fig. 1. The bifurcation diagram of a dynamical system of (3.1) when (a)$P > 0$ and $Q > 0$, and (b) $P > 0$ and $Q < 0$.

3. Qualitative analysis

In this segment, our primary focus is to examine the dynamic characteristics of the two-dimensional system described in Eq. (2.6). Subsequently, we delve into a more comprehensive analysis of the dynamic behavior of two-dimensional dynamical systems by introducing a minor perturbation term

3.1. Bifurcation and phase portrait

In this section, we will explore Eq. (1.1) by utilizing the concept of bifurcation analysis. By the study of Galilean transformation, we change Eq. (2.6) into the planer dynamical system as:

$$\left.\begin{aligned} \frac{d\psi}{d\zeta} &= U, \\ \frac{dU}{d\zeta} &= P\psi - Q\psi^3. \end{aligned}\right\} \tag{3.1}$$

here $P = \frac{1}{\rho}$ and $Q = \frac{\upsilon}{3\rho\omega}$. With the Hamiltonian system,

$$H(\psi, U) = \frac{1}{2}U^2 - \frac{P}{2}\psi^2 + \frac{Q}{4}\psi^4 = h. \tag{3.2}$$

The planner dynamical system (3.1) has three equilibrium points, that are given by

$$a_0(A_0, 0), a_1(A_1, 0), a_2(A_2, 0), \tag{3.3}$$

where $A_0 = 0$, $A_1 = \sqrt{\frac{P}{Q}}$ and $A_2 = -\sqrt{\frac{P}{Q}}$ from jacobian of the system (3.1), obtain the following system.

$$J(U, \psi) = -P + 3Q\psi^2 \tag{3.4}$$

Consequently, the point $(A_0, 0)$ exhibits a saddle-like behavior if $J(a_0) < 0$, indicates a center if $J(a_0) > 0$, and displays a cuspidal point if $J(a_0) = 0$.

At the point $(A_1, 0)$ illustrates a saddle point if $J(a_1) < 0$, shows a center if $J(a_1) > 0$, and represents a cuspidal point if $J(a_1) = 0$.

Similarly, the point $(A_2, 0)$ illustrates a saddle point if $J(a_2) < 0$, shows a center if $J(a_2) > 0$, and represents a cuspidal point if $J(a_2) = 0$.

It is crucial to note that the values for parameters p and Q can be real and are selected precisely. Consequently, we obtain many situations for various conceivable parameter selections, each of which is described in detail (see Fig. 1).

3.2. Chaotic behavior

This section examines Eq.'s quasi-periodic and chaotic dynamics (1.1). To make it more intriguing, a perturbation term $N(\zeta)$ has been introduced into Eq. (3.1). Consequently, the following system can be written using Eq. (3.1) along with the aforementioned perturbed term. The dynamical system that is planar (3.1) and has a perturbation term is capable of being expressed as follows,

$$\left.\begin{aligned} \frac{d\psi}{d\zeta} &= U, \\ \frac{dU}{d\zeta} &= \frac{1}{\rho}\psi - \frac{\upsilon}{3\rho\omega}\psi^3 + N(\zeta). \end{aligned}\right\} \tag{3.5}$$

Where $N(\zeta) = \eta cos(\theta\zeta)$, $Ae^{-0.02\zeta}$ and θ represents the frequency, η denotes the intensity of the perturbed term. Notably, the system (3.5) encompasses an external periodic power that is absent in the system (3.1). The aim is to explore the periodic and chaotic dynamics of Eq. (1.1) under the influence of a disturbance term with undefined parameters. We have effectively predicted the quasi-periodic and turbulent dynamics of the system (3.5) and demonstrated this phenomenon by applying several methods of chaos detection, including time series, Poincaré maps, $2D$ and $3D$ phase portraits, and others.

4. Stability analysis of dynamical system Eq. (1.1)

Consider the perturbed solution of Eq. (1.1) has the form [65]

$$s(x, t) = A_1 + \eta W(x, t). \tag{4.1}$$

It is readily apparent that any constant value A_1 can be identified as a stable state solution for Eq. (1.1). By substitution Eq. (4.1) into Eq. (1.1), we obtained the following result,

$$\eta W_t + \upsilon\eta A_1^2 W_x + \upsilon\eta^3 W^2 W_x + 2A_1\eta^2 W W_x - \rho\eta^3 W_{xxt} = 0. \tag{4.2}$$

Linearization of the Eq. (4.2) gives the following result,

$$W_t + \upsilon A_1^2 W_x = 0. \tag{4.3}$$

Suppose that Eq. (4.3) has solution of the form,

$$w(x, t) = e^{\iota(kx+\eta t)}. \tag{4.4}$$

Solving for η gives us

$$\eta(k) = -\upsilon A_1^2 k. \tag{4.5}$$

This is a dispersion relation, since the real part of Eq. (4.5) is negative for all values then, any superposition of solution will appear to decay, therefore dispersion relation is stable.

4.1. Phase velocity and group velocity

To derive the phase velocity $\frac{\eta(k)}{k}$, we endeavor to obtain a solution that conforms to a specific form.

$$w(x, t) = e^{\iota(kx+\eta t)}. \tag{4.6}$$

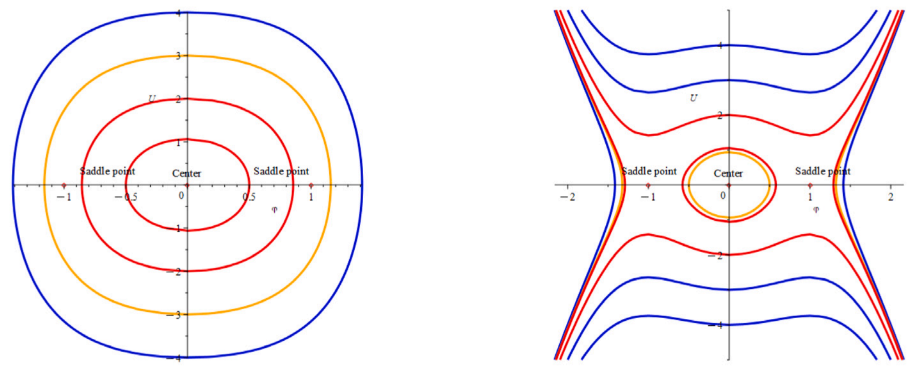

(a) $P<0$and $Q>0$ (b) $P<0$ and$Q<0$

Fig. 2. The bifurcation diagram of a dynamical system (3.1) when (a) $P<0$ and $Q>0$, and (b) $P<0$ and $Q<0$.

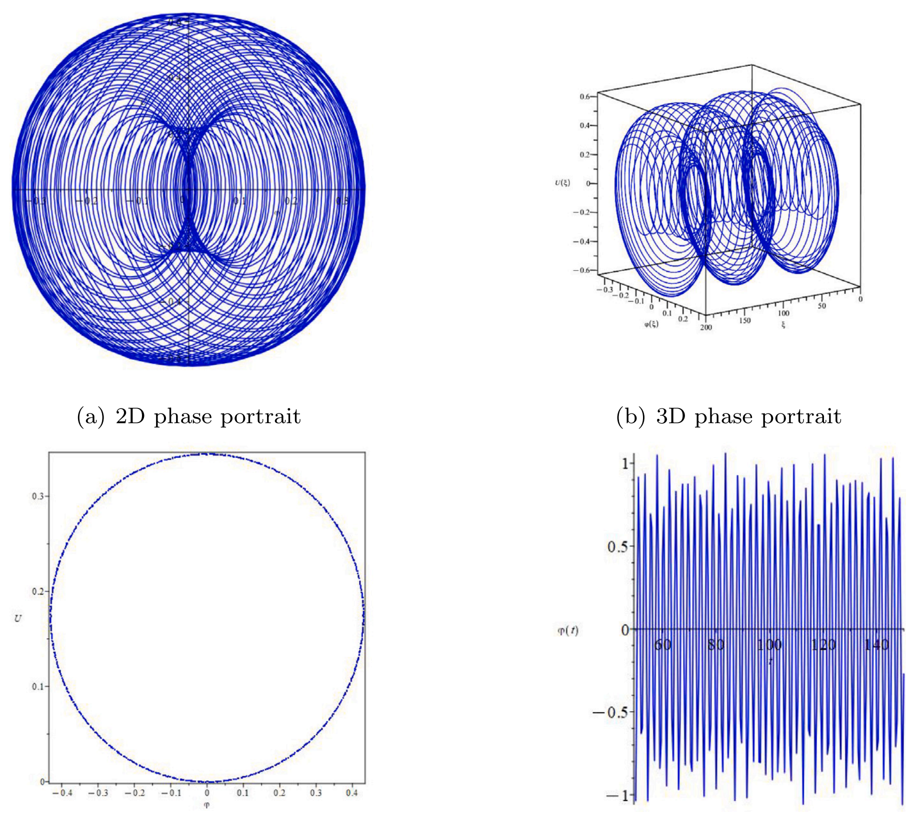

(a) 2D phase portrait (b) 3D phase portrait

(c) Poincaré section (d) Time series

Fig. 3. The graphical visualization of chaotic behaviors for the dynamical system (3.5) with perturbation term $N(\zeta)=0.8\cos(1.2\xi)$.

Substituting the Eq. (4.6) in Eq. (4.5) for solving $\frac{\eta(k)}{k}$, gives us.

$$\frac{\eta(k)}{k}=-\upsilon A_1^2, \tag{4.7}$$

the group velocity, which refers to the velocity at which the energy of a wave packet propagates, exhibits a value that is twice the value of the phase velocity. It is worth noting that the phase velocity is a quantity that varies according to the value of k. Consequently, when a superposition of multiple waves is taken into account, it appears to spread out or disperse.

4.2. Sensitivity analysis of dynamical system Eq. (1.1)

In this part of the research, we investigate the sensitivity analysis of the dynamical system Eq. (1.1) by using the different initial conditions. First, we convert the Eq. (2.6) into two systems of equations by utilizing the Galilean transformation. Let $\psi'=U$ the Eq. (2.6) is converted into the following system [66,67]

$$\left.\begin{aligned}\frac{d\psi}{d\zeta}&=U,\\ \frac{dU}{d\zeta}&=\frac{1}{\rho}\psi-\frac{\upsilon}{3\rho\omega}\psi^3.\end{aligned}\right\} \tag{4.8}$$

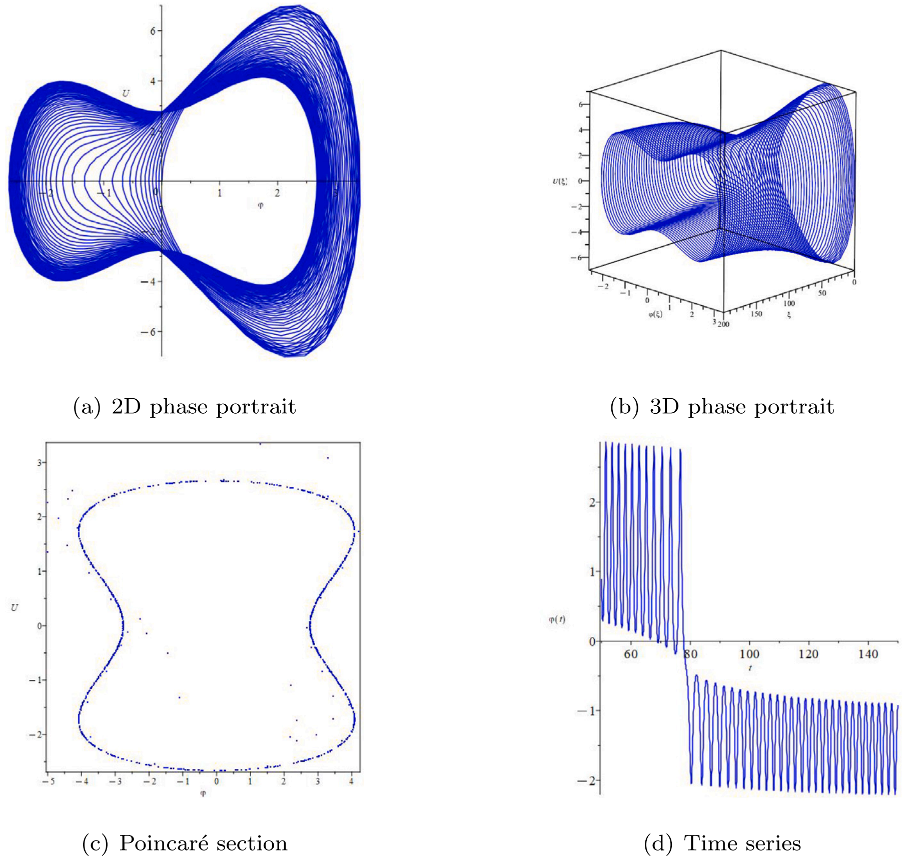

Fig. 4. The graphical visualization of chaotic behaviors for the dynamical system with perturbation term $N(\zeta) = 10e^{-}0.02\zeta$.

Using two different initial conditions, we conduct a detailed sensitivity analysis of the dynamical system (1.1) in this section of the study. The two solutions, using appropriate parameter values like $\rho = 2, \upsilon = 3, \omega = 2$, have been effectively demonstrated in Figs. 6–9. In particular, two solutions are shown in Fig. 6: $(U, \psi) = (0.1, 0)$ in red (solid) and $(U, \psi) = (0.2, 0)$ in navy blue (solid).

Fig. 7 highlights two solutions, namely $(U, \psi) = (0.1, 0)$ in red color (solid) and $(U, \psi) = (0.3, 0)$. In the figure presented in green color, two solutions are shown.

Similarly, Fig. 8 depicts two solutions in the navy blue color solid line and green color solid line, respectively, denoted by $(U, \psi) = (0.2, 0)$ and $(U, \psi) = (0.3, 0)$.

The solutions are compared at initial conditions in Fig. 9. Solid red, $(U, \psi) = (0.1, 0)$; $(U, \psi) = (0.2, 0)$ in the color dash-dot of navy blue and $(U, \psi) = (0.3, 0)$in the color green. A dynamical system's solution may shift slightly in response to small changes in the initial conditions. Stated differently, the two solution curves never intersect under any situation. Thus, we can infer that the governing model exhibits a degree of sensitivity, albeit not excessively sensitive.

5. Structure of soliton solutions

5.1. Modified auxiliary equation method

Following the modified auxiliary equation methodology, we explore the resolution of Eq. (2.3) by considering the subsequent solution in the following manner:

$$\psi(\zeta) = m_0 + \sum_{j=1}^{N} [m_j (g)^{jh(\zeta)} + n_j (g)^{-jh(\zeta)}], \tag{5.1}$$

where m_j, n_j are constants to be determined and $h(\zeta)$ satisfies the following auxiliary equation.

$$h'(\zeta) = \frac{\theta + \eta g^{-h} + \sigma g^{h}}{\ln g}. \tag{5.2}$$

The constants η, θ, σ and g are arbitrary values with $g > 0$, $g \neq 0$. Eq. (5.2) has the following solutions.

• If $\theta^2 - 4\eta\sigma < 0$ and $\sigma \neq 0$, then

$$\begin{aligned} g^{h(\zeta)} &= \frac{-\theta + \sqrt{4\eta\sigma - \theta^2}\tan(\frac{\sqrt{4\eta\sigma-\theta^2}\zeta}{2})}{2\sigma} \quad \text{or} \\ g^{h(\zeta)} &= -\frac{\theta + \sqrt{4\eta\sigma - \theta^2}\cot(\frac{\sqrt{4\eta\sigma-\theta^2}\zeta}{2})}{2\sigma}. \end{aligned} \tag{5.3}$$

• If $\theta^2 - 4\eta\sigma > 0$ and $\sigma \neq 0$, then

$$\begin{aligned} g^{h(\zeta)} &= -\frac{\theta + \sqrt{\theta^2 - 4\eta\sigma}\tanh(\frac{\sqrt{\theta^2-4\eta\sigma}\zeta}{2})}{2\sigma} \quad \text{or} \\ g^{h(\zeta)} &= -\frac{\theta + \sqrt{\theta^2 - 4\eta\sigma}\coth(\frac{\sqrt{\theta^2-4\eta\sigma}\zeta}{2})}{2\sigma}. \end{aligned} \tag{5.4}$$

• If $\theta^2 - 4\eta\sigma = 0$ and $\sigma \neq 0$, then

$$g^{h(\zeta)} = -\frac{2 + \theta\zeta}{2\sigma\zeta}. \tag{5.5}$$

5.2. Utilization of the modified auxiliary equation technique

First of all, we determine the value of the positive integer $N = 1$ using the homogeneous balance principle by comparing the non-linear term with the highest-degree "ψ^3" and the linear term with

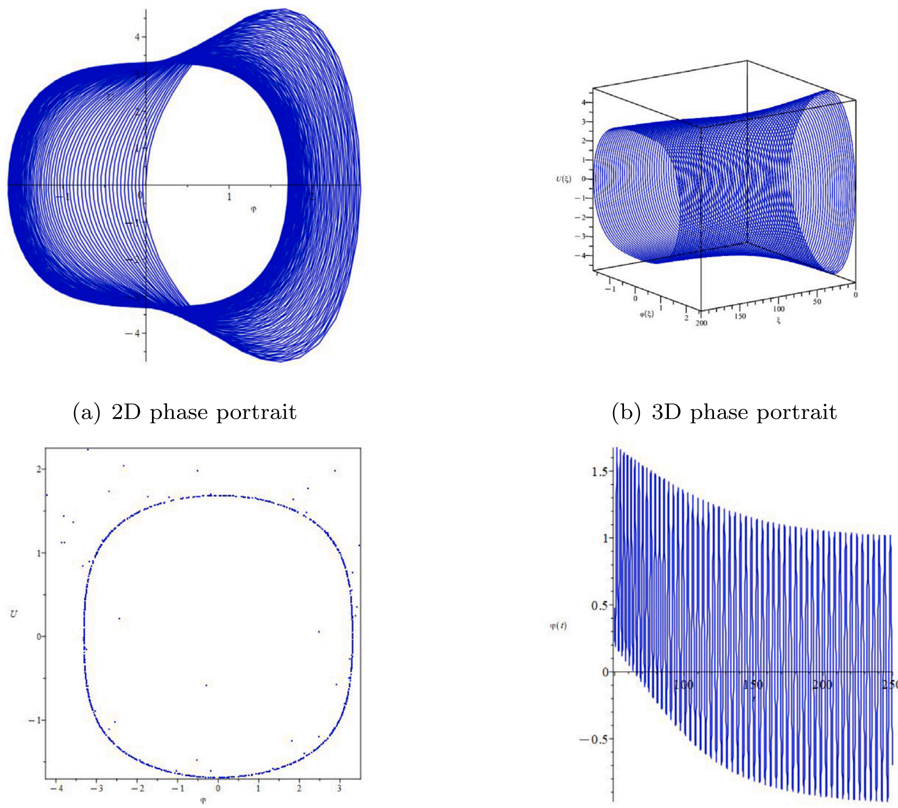

(a) 2D phase portrait   (b) 3D phase portrait

(c) Poincaré section   (d) Time series

Fig. 5. The graphical visualization of chaotic behaviors for the dynamical system with perturbation term $N(\zeta) = 10e^{-}0.02\zeta$.

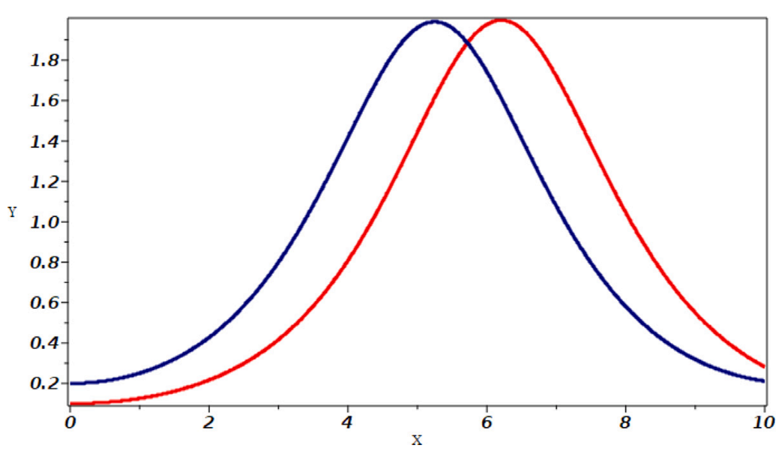

Fig. 6. Sensitivity analysis of the dynamical system Eq. (4.8) by using the different initial conditions such as $(U, \psi) = (0.1, 0)$ in red (solid) and $(U, \psi) = (0.2, 0)$ in navy blue (solid).

highest-order "ψ''" in Eq. (2.6). This is essential for obtaining accurate solutions to Eq. (1.1) through the modified auxiliary equation method.

$$\psi(\zeta) = m_0 + m_1 g^{h(\zeta)} + n_1 g^{-h(\zeta)}. \tag{5.6}$$

By substituting the values from Eq. (5.6) and Eq. (5.2) into Eq. (2.6) and setting the coefficients of different powers of $g^h(\zeta)$ to zero, a system of algebraic equations is derived. By solving this system of equations simultaneously, we obtain the following set of solutions.

Set 1.

$$\omega = \omega, \rho = \frac{2}{4\eta\sigma - \theta^2}, \upsilon = \upsilon, m_0 = \sqrt{-\frac{3\omega}{4\eta\sigma\upsilon - \theta^2\upsilon}}\theta, \tag{5.7}$$

$$m_1 = 2\sqrt{-\frac{3\omega}{4\eta\sigma\upsilon - \theta^2\upsilon}}\sigma, n_1 = 0.$$

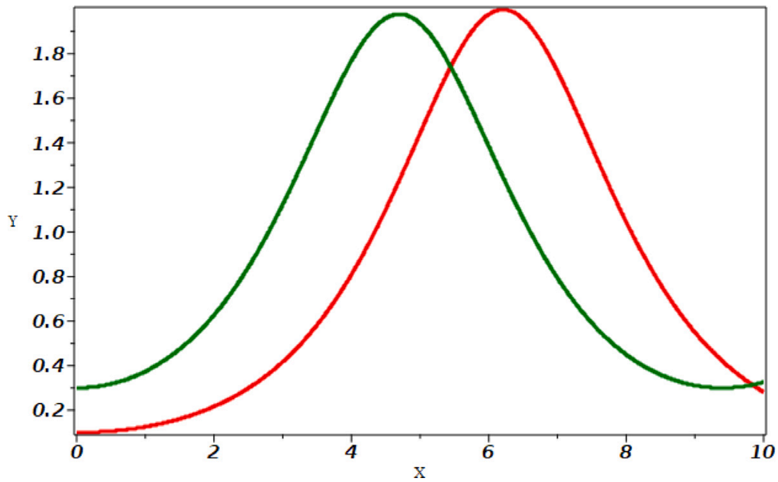

Fig. 7. Sensitivity analysis of the dynamical system Eq. (4.8) by using the different initial conditions such as $(U,\psi) = (0.1, 0)$ in red color (solid) and $(U,\psi) = (0.3, 0)$ in green (solid).

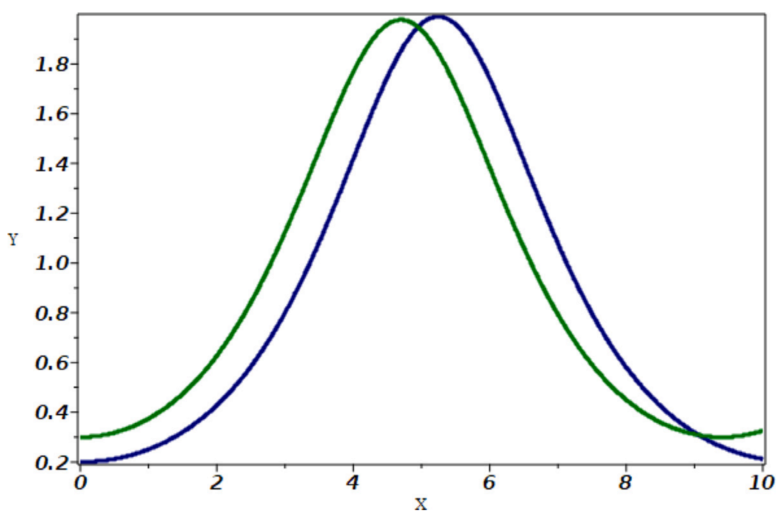

Fig. 8. Sensitivity analysis of the dynamical system Eq. (4.8) by using the different initial conditions such as two solutions in the navy blue color solid line and green color solid line, respectively, denoted by $(U,\psi) = (0.2, 0)$ and $(U,\psi) = (0.3, 0)$.

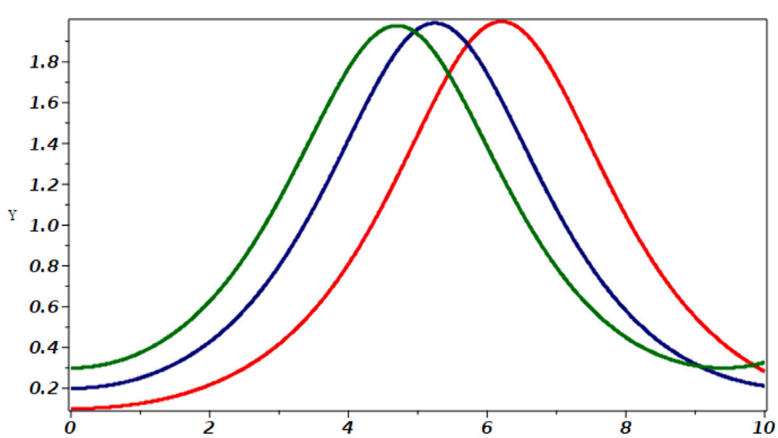

Fig. 9. Sensitivity analysis of the dynamical system Eq. (4.8) by using the different initial conditions such as in three solutions Solid red, $(U,\psi) = (0.1, 0)$; $(U,\psi) = (0.2, 0)$ in the color of navy blue and $(U,\psi) = (0.3, 0)$ in the color green .

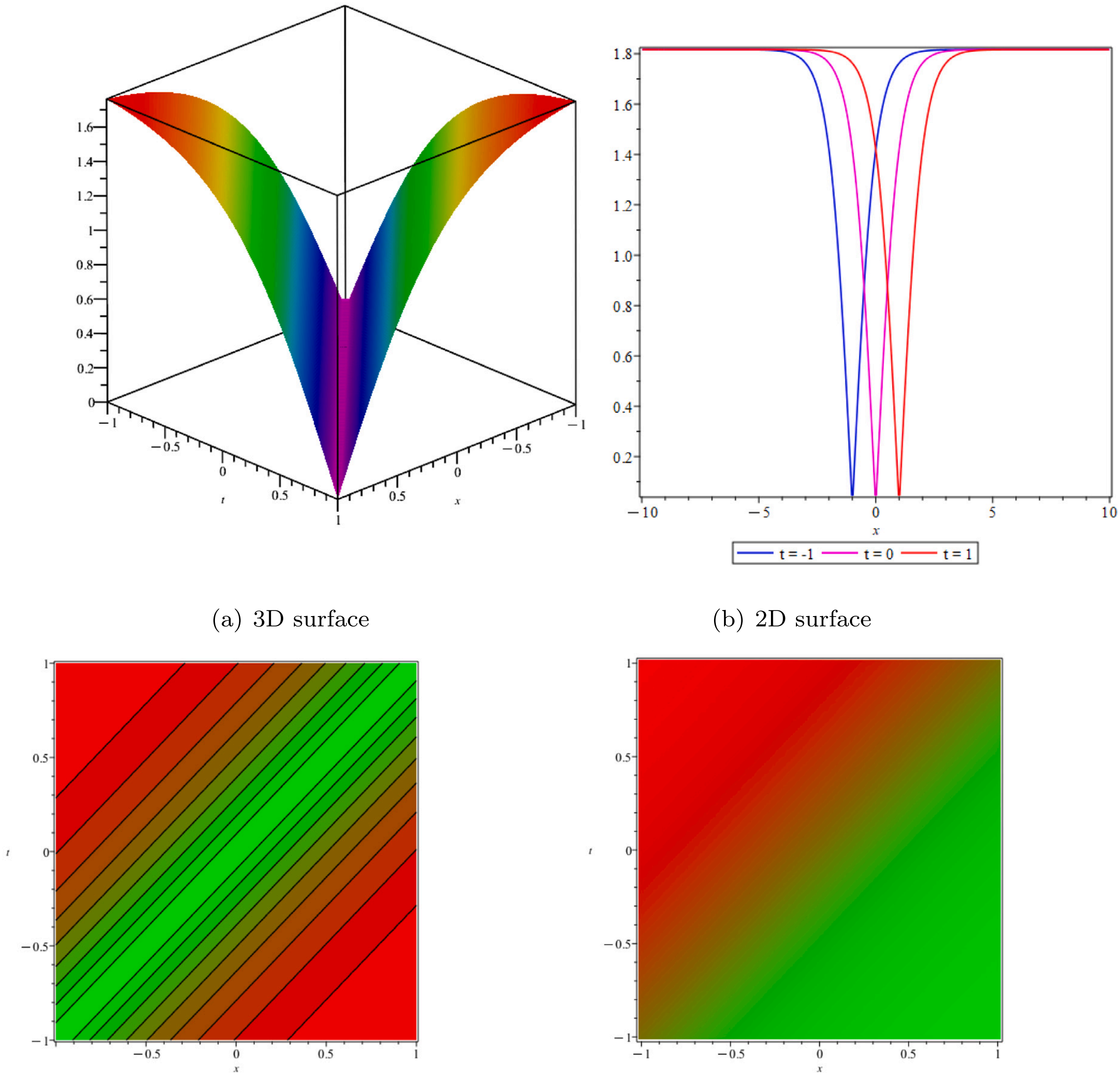

(a) 3D surface (b) 2D surface

(c) Contour plot (d) density plot

Fig. 10. Graphical visualization of derived solution of (5.3) such as (a) 3D surface, (b) 2D surface, (c) contour plot (d) density plot, when $|\psi_1(t,x)| = v = 0.1, \eta = -1, \theta = 2, \sigma = 1, \omega = 0.2, w = 1$.

By utilizing the numerical values attributed to Set 1, we have identified various clusters of solutions to the equation expressed in (1.1).

Family 1.

• When $\theta^2 - 4\eta\sigma < 0$ and $\sigma \neq 0$, then obtain the trigonometric solution.

$$\psi_1(x,t) = \sqrt{-\frac{3\omega}{4\eta\sigma v - \theta^2 v}}\theta + \sqrt{-\frac{3\omega}{4\eta\sigma v - \theta^2 v}}\left(-\theta + \sqrt{4\eta\sigma - \theta^2}\tan\left(\frac{1}{2}\sqrt{4\eta\sigma - \theta^2}\xi\right)\right). \tag{5.8}$$

• When $\theta^2 - 4\eta\sigma > 0$ and $\sigma \neq 0$, then obtain the hyperbolic solution.

$$\psi_2(x,t) = \sqrt{-\frac{3\omega}{4\eta\sigma v - \theta^2 v}}\theta - \sqrt{-\frac{3\omega}{4\eta\sigma v - \theta^2 v}}\left(\theta + \sqrt{-4\eta\sigma + \theta^2}\tanh\left(\frac{1}{2}\sqrt{-4\eta\sigma + \theta^2}\xi\right)\right). \tag{5.9}$$

• When $\theta^2 - 4\eta\sigma = 0$ and $\sigma \neq 0$, then obtain the algebraic solution.

$$\psi_3(x,t) = \sqrt{-\frac{3\omega}{4\eta\sigma v - \theta^2 v}}\theta - \sqrt{-\frac{3\omega}{4\eta\sigma v - \theta^2 v}}\frac{\theta\xi + 2}{\xi}. \tag{5.10}$$

Set 2.

$$\omega = \omega, \rho = \frac{2}{4\eta\sigma - \theta^2}, v = v, m_0 = \sqrt{-\frac{3\omega}{4\eta\sigma v - \theta^2 v}}\theta, m_1 = 0,$$
$$n_1 = 2\sqrt{-\frac{3\omega}{4\eta\sigma v - \theta^2 v}}\eta. \tag{5.11}$$

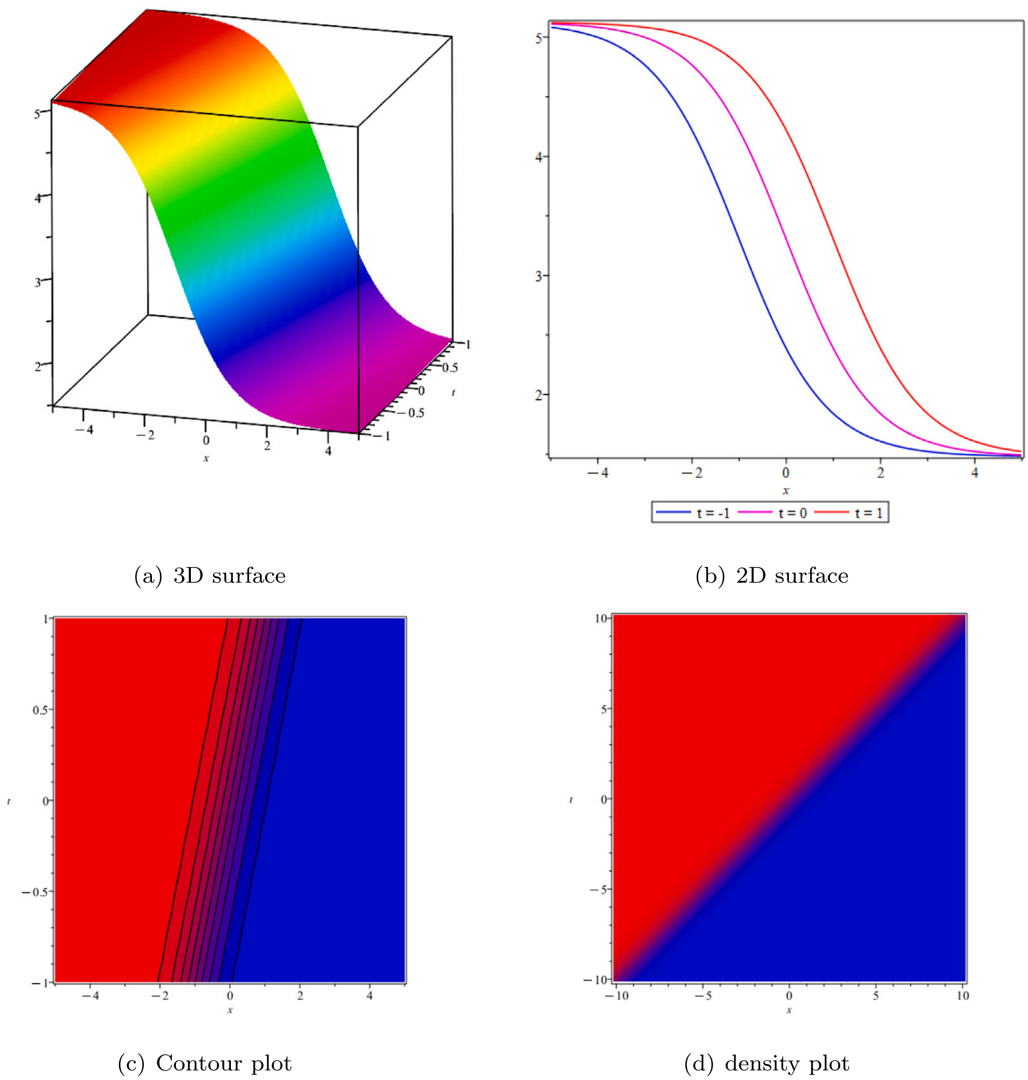

(a) 3D surface (b) 2D surface

(c) Contour plot (d) density plot

Fig. 11. Graphical visualization of derived solution of (5.3) such as (a) 3D surface, (b) 2D surface, (c) contour plot (d) density plot, when $|\psi_2(t,x)| = v = 0.11, \eta = -0.5, \theta = 1, \sigma = 1, \omega = 0.3, w = 1$.

Utilizing the numerical values present in Set 2, we have derived multiple sets of solutions for Eq. (1.1).

Family 2.

• When $\theta^2 - 4\eta\sigma < 0$ and $\sigma \neq 0$, then obtain the trigonometric solution.

$$\psi_4(x,t) = \sqrt{-\frac{3\omega}{4\eta\sigma v - \theta^2 v}}\theta + \frac{4\sqrt{-\frac{3\omega}{4\eta\sigma v-\theta^2 v}}\eta\sigma}{-\theta + \sqrt{4\eta\sigma - \theta^2}\tan\left(\frac{1}{2}\sqrt{4\eta\sigma - \theta^2}\xi\right)}. \tag{5.12}$$

• When $\theta^2 - 4\eta\sigma > 0$ and $\sigma \neq 0$, then obtain the hyperbolic solution.

$$\psi_5(x,t) = \sqrt{-\frac{3\omega}{4\eta\sigma v - \theta^2 v}}\theta - \frac{4\sqrt{-\frac{3\omega}{4\eta\sigma v-\theta^2 v}}\eta\sigma}{\theta + \sqrt{-4\eta\sigma + \theta^2}\tanh\left(\frac{1}{2}\sqrt{-4\eta\sigma + \theta^2}\xi\right)}. \tag{5.13}$$

• When $\theta^2 - 4\eta\sigma = 0$ and $\sigma \neq 0$, then obtain the algebraic solution.

$$\psi_6(x,t) = \sqrt{-\frac{3\omega}{4\eta\sigma v - \theta^2 v}}\theta - \frac{4\sqrt{-\frac{3\omega}{4\eta\sigma v-\theta^2 v}}\eta\sigma\xi}{\theta\xi + 2}. \tag{5.14}$$

6. Graphical representation

In this specific section of the manuscript, we examine the graphical characteristics of the various obtained solutions. It is essential to assign suitable values to the arbitrary constants to produce clearly defined visual representations of the solutions in 3D, 2D, contour plots, and density plots.

Part (a) of the figures illustrates a 3D surface plot depicting the traveling wave behavior. Section (b) presents a 2D surface plot displaying the variation of the wave behavior for different values of t. The figures in section (b) utilize contour plots to visually convey the structural composition of the solutions, and part (d) shows the density plot of the derived solutions.

Fig. 10 indicates the behavior of dark soliton with suitable parameter values when $|\psi_1(t,x)| = v = 0.1, \eta = -1, \theta = 2, \sigma = 1, \omega = 0.2, w = 1$.

Fig. 11 depicts the kink soliton with different parameter values when $|\psi_2(t,x)| = v = 0.11, \eta = -0.5, \theta = 1, \sigma = 1, \omega = 0.3, w = 1$.

Fig. 12 shows the behavior of kink wave solution with different parameter values when $|\psi_4(t,x)| = v = 0.06, \eta = 3, \theta = 2, \sigma = 1, \omega = 0.03, w = 0.5$.

Fig. 13 shows the behavior of singular soliton solution with different parameter values when $|\psi_5(t,x)| = v = 2, \eta = -0.1, \theta = -2, \sigma = 1, \omega = 0.3, w = 1$.

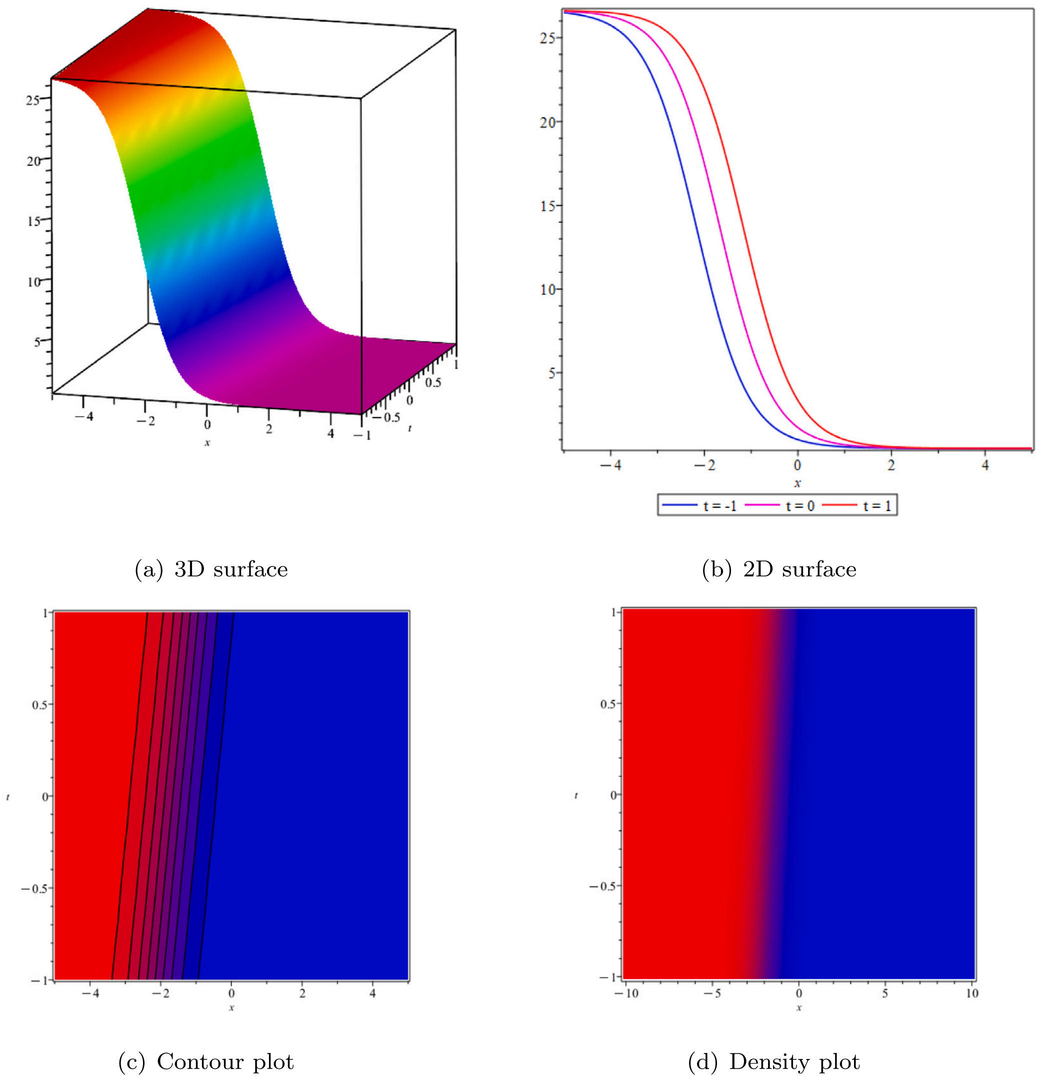

(a) 3D surface (b) 2D surface

(c) Contour plot (d) Density plot

Fig. 12. Graphical visualization of derived solution of (5.3) such as (a) 3D surface, (b) 2D surface, (c) contour plot (d) density plot, when $|\psi_4(t,x)| = v = 0.06, \eta = 3, \theta = 2, \sigma = 1, \omega = 0.03, w = 0.5$.

7. Conclusion

In this manuscript, we have analyzed the nonlinear characteristics of wave propagation to the (1+1)-dimensional modified equal width equation (MEWE) that is used to simulate the one-dimensional wave propagation nonlinear media, incorporating the dispersion process. By applying the traveling wave transformation, we converted the NLPDES into ODEs. Using the Galilean transformations Eq. (2.6) was converted into a coupled planar dynamical system and qualitative analysis was investigated. First, bifurcation analysis of the system Eq. (5.2) has been analyzed. Phase portraits of the bifurcation analysis are represented at equilibrium points of the planar dynamical system shown in Fig. 2. We have investigated many approaches for identifying chaos, which is defined as its random and unpredictable nature, in self-regulating dynamic systems to illustrate the chaotic tendencies inside the perturbed dynamic system. As shown in (Figs. 3, 4, 5), these techniques include the use of time series, Poincaré maps, $2D$ and $3D$ phase portraits, and time series. . Furthermore, a thorough presentation of the sensitivity and stability analysis for a range of initial conditions has been provided, demonstrating the intrinsic stability of the system under investigation. This is demonstrated by the fact that abrupt changes in the solutions do not occur from even little perturbations in the initial circumstances, as illustrated in (Figs. 6, 7, 8, 9). By applying efficient techniques to find the exact soliton solutions known as the modified auxiliary equation method. Utilizing this technique in Eq. (2.6), we see the different types of solutions like trigonometric, hyperbolic, and rational solutions These new findings demonstrate the role of the MEW equation, which opens the door to a more complete description of nonlinear dynamical systems and soliton theory.

CRediT authorship contribution statement

Syed Asif Ali Shah: Writing – original draft, Formal analysis, Conceptualization. **Ejaz Hussain:** Writing – review & editing, Validation, Software, Resources, Methodology, Formal analysis, Conceptualization. **Wen-Xiu Ma:** Visualization, Validation, Supervision, Project administration. **Zhao Li:** Visualization, Formal analysis, Conceptualization. **Adham E. Ragab:** Validation, Investigation, Formal analysis, Data curation. **Tamer M. Khalaf:** Resources, Validation, Visualization.

Declaration of competing interest

I declare that we have no competing interest in publishing this article on behalf of all the authors.

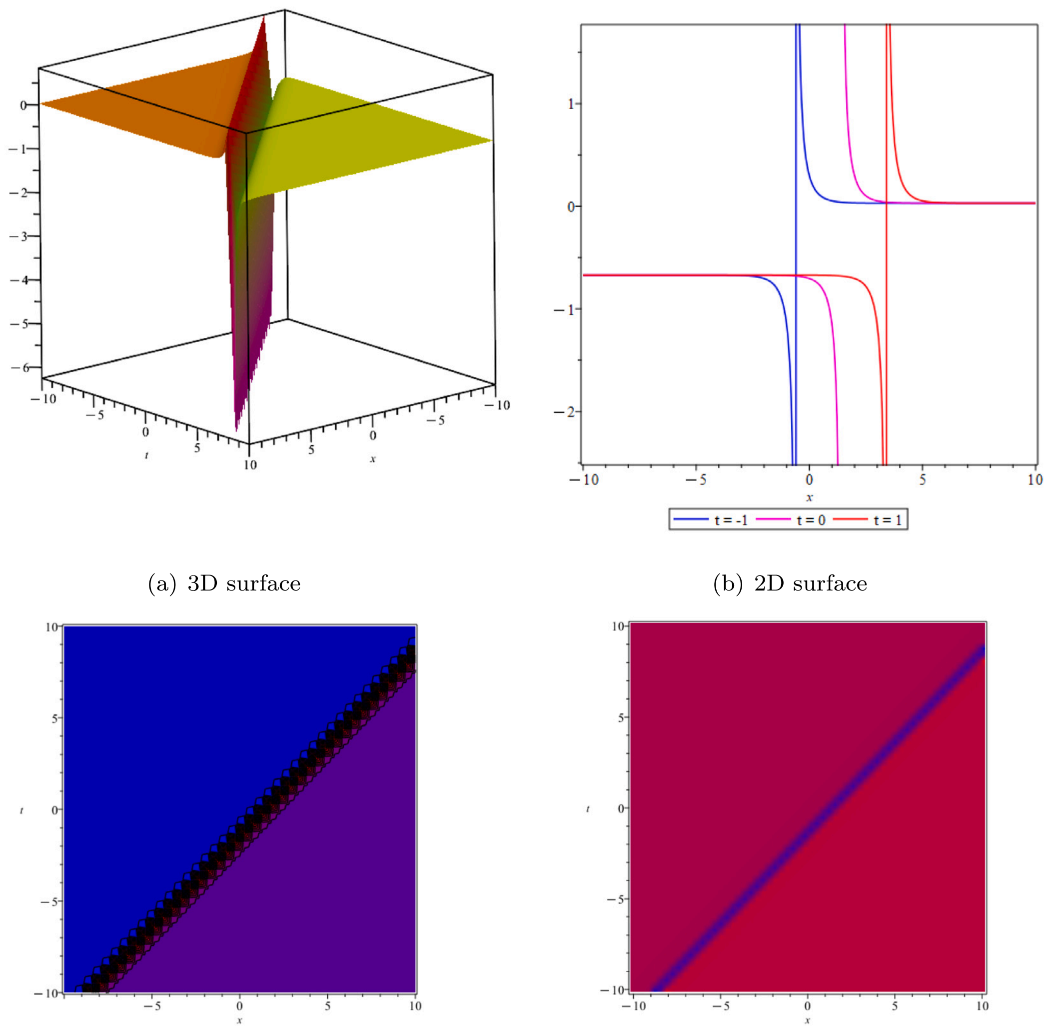

(a) 3D surface (b) 2D surface

(c) Contour plot (d) Contour plot

Fig. 13. Graphical visualization of derived solution of (5.3) such as (a) 3D surface, (b) 2D surface, (c) contour plot (d) density plot, when $|\psi_5(t,x)| = v = 2, \eta = -0.1, \theta = -2, \sigma = 1, \omega = 0.3, w = 1$.

Data availability

Data will be made available on request.

Acknowledgments

The authors extend their appreciation to the King Saud University, Saudi Arabia for funding this work through the Researchers Supporting Project number (RSPD2024R970), King Saud University, Riyadh, Saudi Arabia

Funding

This research was funded by King Saud University, Saudi Arabia, Project No. (RSPD2024R970).

References

[1] Ahmad Hijaz, Khan Tufail A, Stanimirovic Predrag S, Shatanawi Wasfi, Botmart Thongchai. New approach on conventional solutions to nonlinear partial differential equations describing physical phenomena. Results Phys 2022;41:105936.
[2] Alam M Nur, Bonyah Ebenezer, Fayz-Al-Asad Md, Osman MS, Abualnaja Kholod M. Stable and functional solutions of the Klein-Fock-Gordon equation with nonlinear physical phenomena. Phys Scr 2021;96(5):055207.
[3] Yusuf Abdullahi, Sulaiman Tukur Abdulkadir, Hincal Evren, Baleanu Dumitru. Lump, its interaction phenomena and conservation laws to a nonlinear mathematical model. J Ocean Eng Sci 2022;7(4):363–71.
[4] Aktürk Tolga, Kubal Çağlar. The behavior of plasma and space-charge waves represented by nonlinear mathematical models. J Ocean Eng Sci 2022.
[5] Rezazadeh Hadi. New solitons solutions of the complex Ginzburg–Landau equation with Kerr law nonlinearity. Optik 2018;167:218–27.
[6] Hussain Ejaz, Shah Syed Asif Ali, Bariq Abdul, Li Zhao, Ahmad Muhammad Riaz, Ragab Adham E, et al. Solitonic solutions and stability analysis of Benjamin Bona Mahony Burger equation using two versatile techniques. Sci Rep 2024;14(1):13520.
[7] Attaullah Muhammad Shakeel, Shah Nehad Ali, Chung Jae Dong. Modified exp-function method to find exact solutions of ionic currents along microtubules. Mathematics 2022;10(6):851.
[8] Fadhal Emad, Akbulut Arzu, Kaplan Melike, Awadalla Muath, Abuasbeh Kinda. Extraction of exact solutions of higher order Sasa-Satsuma equation in the sense of beta derivative. Symmetry 2022;14(11):2390.
[9] Raza Nauman, Seadawy Aly R, Kaplan Melike, Butt Asma Rashid. Symbolic computation and sensitivity analysis of nonlinear Kudryashov's dynamical equation with applications. Phys Scr 2021;96(10):105216.
[10] Ma Wen-Xiu. The inverse scattering transform and soliton solutions of a combined modified Korteweg–de Vries equation. J Math Anal Appl 2019;471(1–2):796–811.
[11] Javid Ahmad, Raza Nauman, Osman MS. Multi-solitons of thermophoretic motion equation depicting the wrinkle propagation in substrate-supported graphene sheets. Commun Theor Phys (Beijing) 2019;71(4):362.
[12] Ma Wen-Xiu. N-soliton solution and the Hirota condition of a (2+ 1)-dimensional combined equation. Math Comput Simulation 2021;190:270–9.

[13] Shatat Feras. Soliton solutions for Fisher equation by using simplified Hirota's method. J Phys Conf Ser 2018;1132(1):012015.

[14] Yin Yu-Hang, Lü Xing, Ma Wen-Xiu. Bäcklund transformation, exact solutions and diverse interaction phenomena to a (3+ 1)-dimensional nonlinear evolution equation. Nonlinear Dynam 2022;108(4):4181–94.

[15] Ma Wen-Xiu. Binary darboux transformation of vector nonlocal reverse-time integrable nls equations. Chaos Solitons Fractals 2024;180:114539.

[16] Ma Wen-Xiu, Yehui Huang, Fudong Wang, Yong Zhang, Liyuan Ding. Binary darboux transformation of vector nonlocal reverse-space nonlinear schrödinger equations. Int J Geom Methods Mod Phys 2024;21:2450182.

[17] Khater Mostafa MA, Lu Dianchen, Attia Raghda AM. Lump soliton wave solutions for the (2+ 1)-dimensional Konopelchenko–Dubrovsky equation and KdV equation. Modern Phys Lett B 2019;33(18):1950199.

[18] Kaplan Melike, Akbulut Arzu. A mathematical analysis of a model involving an integrable equation for wave packet envelope. J Math Univ Tokushima 2022;2022.

[19] Kaplan Melike, Akbulut Arzu. The analysis of the soliton-type solutions of conformable equations by using generalized Kudryashov method. Opt Quantum Electron 2021;53:1–21.

[20] Kaplan Melike, Akbulut Arzu. The analysis of the soliton-type solutions of conformable equations by using generalized Kudryashov method. Opt Quantum Electron 2021;53:1–21.

[21] Rafiq Muhammad Hamza, Jhangeer Adil, Raza Nauman. The analysis of solitonic, super nonlinear, periodic, quasiperiodic, bifurcation and chaotic patterns of perturbed Gerdjikov–Ivanov model with full nonlinearity. Commun Nonlinear Sci Numer Simul 2023;116:106818.

[22] Ibrahim Israa A, Taha Wafaa M, Noorani MSM. Homogenous balance method for solving exact solutions of the nonlinear Benny-Luke equation and Vakhnenko-Parkes equation. Zanco J Pure Appl Sci 2019;31:52–6.

[23] Zhang Hao, Jing Min, Dong Shuai, Dachu Dong Ye Liu, Meng Yongpeng. Stability and evolutionary trend of hopf bifurcations in double-input SEPIC DC–DC converters. Int J Bifurcation Chaos 2019;29(14):1950192.

[24] Tang Lu. Bifurcation analysis and multiple solitons in birefringent fibers with coupled Schrödinger-Hirota equation. Chaos Solitons Fractals 2022;161:112383.

[25] Tang Lu. Dynamical behavior and multiple optical solitons for the fractional Ginzburg–Landau equation with β-derivative in optical fibers. Opt Quantum Electron 2024;56(2):175.

[26] Tang Lu. Bifurcation analysis and optical soliton solutions for the fractional complex Ginzburg–Landau equation in communication systems. Optik 2023;276:170639.

[27] Tang Lu, Biswas Anjan, Yıldırım Yakup, Aphane Maggie, Alghamdi Abdulah A. Bifurcation analysis and optical soliton perturbation with Radhakrishnan–Kundu–Lakshmanan equation. Proc Est Acad Sci 2024;73(1).

[28] Tang Lu. Optical solitons perturbation and traveling wave solutions in magneto-optic waveguides with the generalized stochastic Schrödinger–Hirota equation. Opt Quantum Electron 2024;56(5):773.

[29] Tang Lu, Biswas Anjan, Yıldırım Yakup, Alghamdi Abdulah A. Bifurcation analysis and optical solitons for the concatenation model. Phys Lett A 2023;480:128943.

[30] Wazwaz Abdul-Majid, Osman Mohamed S. Analyzing the combined multi-waves polynomial solutions in a two-layer-liquid medium. Comput Math Appl 2018;76(2):276–83.

[31] Chen Yu-Qiong, Tang Yu-Hao, Manafian Jalil, Rezazadeh Hadi, Osman MS. Dark wave, rogue wave and perturbation solutions of Ivancevic option pricing model. Nonlinear Dynam 2021;105:2539–48.

[32] Osman MS. Multi-soliton rational solutions for quantum Zakharov-Kuznetsov equation in quantum magnetoplasmas. Waves Random Complex Media 2016;26(4):434–43.

[33] Kumar S, Dhiman SK, Baleanu D, Osman MS, Wazwaz AM. Lie symmetries, closed-form solutions and various dynamical profiles of solitons for the variable coefficient (2+ 1)-dimensional KP equations. Symmetry 2022;14:597, Crossref, Web of Science.

[34] Iqbal Md Ashik, Ganie Abdul Hamid, Miah Md Mamun, Osman Mohamed S. Extracting the ultimate new soliton solutions of some nonlinear time fractional PDEs via the conformable fractional derivative. Fract Fractional 2024;8(4):210.

[35] Hossain Md Nur, Miah M Mamun, Ganie Abdul Hamid, Osman MS, Ma Wen-Xiu. Discovering new abundant optical solutions for the resonant nonlinear Schrödinger equation using an analytical technique. Opt Quantum Electron 2024;56(5):847.

[36] Chakrabarty Anuz Kumar, Roshid Md Mamunur, Rahaman MM, Abdeljawad Thabet, Osman MS. Dynamical analysis of optical soliton solutions for CGL equation with Kerr law nonlinearity in classical, truncated m-fractional derivative, beta fractional derivative, and conformable fractional derivative types. Results Phys 2024;60:107636.

[37] Faridi Waqas Ali, Iqbal Mujahid, Ramzan Bilal, AlQahtani Salman A, Osman MS, Akinyemi Lanre, et al. The formation of invariant optical soliton structures to electric-signal in the telegraph lines on basis of the tunnel diode and chaos visualization, conserved quantities: Lie point symmetry approach. Optik 2024;305:171785.

[38] Hosseini K, Alizadeh F, Hinçal E, Kaymakamzade B, Dehingia K, Osman MS. A generalized nonlinear Schrödinger equation with logarithmic nonlinearity and its Gaussian solitary wave. Opt Quantum Electron 2024;56(6):929.

[39] Ma Wen-Xiu. Type (λ^{*},λ) reduced nonlocal integrable akns equations and their soliton solutions. Appl Numer Math 2024;119:105–13.

[40] Liu Jinxing, Nadeem Muhammad, Osman MS, Alsayaad Yahya. Study of multi-dimensional problems arising in wave propagation using a hybrid scheme. Sci Rep 2024;14(1):5839.

[41] Akinyemi Lanre, Hosseini Kamyar, Salahshour Soheil. The bright and singular solitons of (2+ 1)-dimensional nonlinear Schrödinger equation with spatio-temporal dispersions. Optik 2021;242:167120.

[42] Raza Nauman, Kaplan Melike, Javid Ahmad, Inc Mustafa. Complexiton and resonant multi-solitons of a (4+ 1)-dimensional Boiti–Leon–Manna–Pempinelli equation. Opt Quantum Electron 2022;54:1–16.

[43] Wazwaz Abdul-Majid. Two B-type Kadomtsev–Petviashvili equations of (2+ 1) and (3+ 1) dimensions: multiple soliton solutions, rational solutions, and periodic solutions. Comput Fluids 2013;86:357–62.

[44] Feng Lian-Li, Zhang Tian-Tian. Breather wave, rogue wave and solitary wave solutions of a coupled nonlinear Schrödinger equation. Appl Math Lett 2018;78:133–40.

[45] Wazwaz Abdul-Majid. Multiple kink solutions for two coupled integrable (2+ 1)-dimensional systems. Appl Math Lett 2016;58:1–6.

[46] Ismael Hajar F, Sulaiman Tukur Abdulkadir, Nabi Harivan R, Shah Nehad Ali, Botmart Thongchai. Multiple soliton, M-lump, and interaction solutions to the (3+ 1)-dimensional soliton equation. Results Phys 2023;45:106220.

[47] Ma Wen-Xiu, Jin-Yun Yang. Four-component liouville integrable models and their bi-hamiltonian formulations. Rom J Phys 2024;69(1-2):101.

[48] Ma Wen-Xiu. Integrable couplings and two-dimensional unital algebras. Axioms 2024;13(8):481.

[49] Strogatz Steven H. Nonlinear dynamics and chaos with student solutions manual: with applications to physics, biology, chemistry, and engineering. CRC Press; 2018.

[50] David Ruelle. Elements of differentiable dynamics and bifurcation theory. Elsevier; 2014.

[51] Alidousti Javad. Stability and bifurcation analysis for a fractional prey–predator scavenger model. Appl Math Model 2020;81:342–55.

[52] Ma Wen-Xiu. A combined liouville integrable hierarchy associated with a fourth-order matrix spectral problem. Commun Theoret Phys 2024;76(7):075001.

[53] Ma Wen-Xiu. Four-component combined integrable equations possessing bi-hamiltonian formulations. Modern Phys Lett B 2024;38:2450319.

[54] Ruelle David. Elements of differentiable dynamics and bifurcation theory. Elsevier; 2014.

[55] Wazwaz Abdul-Majid. The tanh and the sine–cosine methods for a reliable treatment of the modified equal width equation and its variants. Commun Nonlinear Sci Numer Simul 2006;11(2):148–60.

[56] Lu Junfeng. He's variational iteration method for the modified equal width equation. Chaos Solitons Fractals 2009;39(5):2102–9.

[57] Esen AL, Kutluay SE. Solitary wave solutions of the modified equal width wave equation. Commun Nonlinear Sci Numer Simul 2008;13(8):1538–46.

[58] Esen AL. A lumped Galerkin method for the numerical solution of the modified equal-width wave equation using quadratic B-splines. Int J Comput Math 2006;83(5–6):449–59.

[59] Rui Weiguo, Xie Shaolong, Long Yao, He Bin. Integral bifurcation method and its application for solving the modified equal width wave equation and its variants. In: Rostocker mathematisches kolloquium. vol. 62, 2007, p. 87–106.

[60] Saboor Abdul, Shakeel Muhammad, Liu Xinge, Zafar Asim, Ashraf Muhammad. A comparative study of two fractional nonlinear optical model via modified $((\frac{G'}{G^2}))$-expansion method. Opt Quantum Electron 2024;56(2):259.

[61] Yokuş Asıf, Durur Hülya, Nofal Taher A, Abu-Zinadah Hanaa, Tuz Münevver, Ahmad Hijaz. Study on the applications of two analytical methods for the construction of traveling wave solutions of the modified equal width equation. Open Phys 2020;18(1):1003–10.

[62] Hassan Hany N. An accurate numerical solution for the modified equal width wave equation using the Fourier pseudo-spectral method. J Appl Math Phys 2016;4(6):1054–67.

[63] Biazar J, Ayati Z, Ebrahimi H. New solitonary solutions for modified equal-width wave equations using exp-function method. Int J Nonlin Dyn Eng Sci 2009;1:109–14.

[64] Wang Heng, Chen Longwei, Wang Hanquan. Exact travelling wave solutions of the modified equal width equation via the dynamical system method. Nonlin Anal Differ Equ 2016;4:9–15.

[65] Mahmood Irfan, Hussain Ejaz, Mahmood Asif, Anjum Arfan, Shah Syed Asif Ali. Optical soliton propagation in the Benjamin–Bona–Mahoney–Peregrine equation using two analytical schemes. Optik 2023;287:171099.

[66] Hussain Ejaz, Mutlib Abdul, Li Zhao, Ragab Adham E, Shah Syed Asif Ai, Az-Zo'bi Emad A, et al. Theoretical examination of solitary waves for Sharma–Tasso–Olver Burger equation by stability and sensitivity analysis. Z Angew Math Phys 2024;75(3):96.

[67] Hussain Ejaz, Li Zhao, Shah Syed Asif Ali, Az-Zo'bi Emad A, Hussien Mohamed. Dynamics study of stability analysis, sensitivity insights and precise soliton solutions of the nonlinear (STO)-Burger equation. Opt Quantum Electron 2023;55(14):1274.